Reversal of Arctic Oscillation pattern and its relation to extreme hot summer in Japan in 2010

Climate and Ecosystems Dynamics Division

Department of Environmental Science & Technology

Mie University

507322

Yuriko Otomi

Supervisor: **Prof. Yoshihiro Tachibana**

March 1, 2011

Contents

Abstract

In 2010, Japan experienced abnormal hot summer nationwide. The abnormal hot summer was planetary scale. In retrospect, on the other hand, just a half year before the hottest summer, in the winter of 2009/2010, Eurasian continent had suffered from anomalous cold winter in association with record breaking negative Arctic Oscillation (AO). The AO (SV NAM) index defined by *Ogi et al.* (2004) consistently continued negative from December 2009 to Jun 2010, but it jumped to anomalous positive in the beginning of summer. The abrupt change of the AO index in 2010 could capture both abnormal cold winter and abnormal hot summer in 2010. Here, we hypothesized the winter anomalous negative AO influenced the summer anomalous positive AO through the oceanic memory. The purpose of this study is to confirm the hypothesis.

We could successfully confirm the each process related to the hypothesis. We could find the possibility that the strong winter negative AO influenced summer abnormal weather in association with the summer positive AO. The hemispheric scale atmospheric anomalous pattern in winter remotely influences hemispheric scale summer weather. On other hand, it means that high and mid latitude of wintertime influenced the region of low latitude, and the effect against bounced high and mid latitude of summertime.

Chapter 1 Introduction

In 2010, Japan experienced abnormally hot summer nationwide. In particular, the summer averaged temperature of northern and eastern parts of Japan severely exceeded from the normal. According to Japan Meteorological Agency (JMA), some weather stations there recorded the highest temperature since modern weather observational system started in 1946. Many observatories exceeded the normal by more than 2℃ in the North Japan. The 55 observatories in Japan update the maximum of the average temperature of summer. The abnormal hot summer was planetary scale. Summer temperatures in Europe, in particular, in Moscow, were record breaking hot. In retrospect, on the other hand, just a half year before the hottest summer, i.e., in the winter of 2009/2010, Eurasian continent had suffered from anomalous cold winter in association with record breaking negative Arctic Oscillation (AO), which showed positive sea level pressure anomalies over the Arctic and positive over the mid-latitudes. The AO index of December 2009 was negatively largest in the past 30 years (*Wang and Chen*, 2010). The drastic jump from the coldest winter to the hottest summer has been preserving in our memory. Not only is the memory preserved in our mind, but also may the memory be preserved in somewhere on the earth. If the memory of the anomalous negative wintertime AO in 2009/2010 was preserved in an ocean, this dormant memory in the ocean may be called up in the following summer because of its large thermal heat capacity.

Figure 1 shows the winter-to-summer evolution of the AO index by *Ogi et al.* (2004), whose detailed explanation is described in the later chapter. The index exhibits anomalous negative AO index in the winter of 2009/2010 and it jumped to anomalous positive in the beginning of summer, and then this anomalous positive index lasted to the beginning of August. The summer time anomalous positive AO is related to the occurrence of blocking anticyclone in association with abnormal hot summer in Europe (*Tachibana et al.*, 2010). Therefore, the abrupt change of the AO index in 2010 could capture both the abnormal cold winter and abnormal hot summer in 2010.

Here, we introduce our hypothesis that the wintertime anomalous negative AO influenced the summertime anomalous positive AO through the oceanic memory. *Tanimoto and Xie* (2002) pointed out that winter negative North Atlantic Oscillation (NAO) does not cool down sea surface temperature (SST) on the region in the low latitude of the Atlantic. Because the horizontal structure of the NAO and the AO in the Atlantic sector is similar, wintertime large negative AO will keep the SST of this region warm. Because the thermal heat capacity of the ocean is large, the warmer SST condition will maintain until following spring and summer. Warmer SST in the following summer, in reverse, can heat the atmosphere. This tropical SST influence upon the atmosphere remotely will influence the mid-latitude upper air through Rossby wave propagation. The jet stream then will meander by this wave forcing. The blocking anticyclone will be formed by meandering of the jet. The summer time anomalous positive AO is related to the occurrence of blocking anticyclone (*Tachibana et al.*, 2010). By this process, the pressure pattern of the negative AO continued for a long time. The purpose of this study is to confirm the hypothesis.

We can forecast global abnormal hot summer from previous winter if global abnormal heat is related with winter AO. The forecast can contribute to Japanese and global economy, agricultural, and fishery industries if we can forecast global abnormal heat early. Therefore, we examined the relation between the winter negative AO and the summer positive AO, and the influence that the abrupt change of the AO index gave global and Japanese abnormal hot summer of 2010.

Chapter 2 Data and method

The seasonal variations of the Northern Hemisphere annular mode (SV NAM) were developed by *Ogi et al.* (2004), which determined the SV NAM by an empirical orthogonal function (EOF) analysis of a temporal covariance matrix of geopotential height fields for individual calendar months, using zonally averaged monthly geopotential height field from 1000-hPa to 200-hPa for the area poleward of 40˚N. SV NAM well accords with AO in winter, but does not accord with AO in summer (e.g., *Ogi et al.*, 2004, *Tachbana et al.*, 2010). *Ogi et al.* (2005) and *Tachibana et al.* (2010) demonstrated that SV NAM successfully captures summertime anomalous weathers in association with blocking anticyclones, such as hot summer in Europe in 2003, whereas original AO defined by *Thompson and Wallace* (2000) could not capture such a hot summer. We therefore use SV NAM index in this study. To avoid the confusion for the terminology between the original AO and the SV NAM, this study refers the SV NAM index as AO index. The daily time series of the AO index is from the projection of daily zonal mean geopotential height anomalies onto the EOF in each month. The time series of the AO index shown in Figure 1 was calculated by this method.

Daily data of geopotential height, temperature and wind velocity from the National Centers for Environmental Prediction/National Center for Atmospheric Research (NCEP/NCAR) reanalysis dataset (*Kalnay et al.*, 1996) were used to analyze the large-scale atmospheric fields and determine SV NAM index. The spatial resolution is global grid of 2.5° of latitude and 2.5° of longitude. Daily and monthly means of velocity potential from NCEP/NCAR reanalysis dataset were also used to analyze the convection and the divergence of the atmosphere. The spatial resolution is T62 Gaussian grid with 192×94 points. These data cover the period from 1958 to 2010 in this study.

Daily and monthly means of outgoing longwave radiation (OLR) data were provided by interpolated OLR of the National Oceanic and Atmospheric Administration (NOAA)/OAR/ESRL PSD (*Liebmann and Smith*, 1996). The spatial resolution is global grid of 2.5° of latitude and 2.5° of longitude. The data coverage used in this study is the period from June 1974 to November 2010, except for March to December 1978, which is unavailable to satellite failure.

Monthly means of SST data were provided by NOAA_ERSST_V3 data of the NOAA/OAR/ESRL PSD (*Smith et al.*, 2008 and *Xue et al.,* 2003). The spatial resolution is global grid of 2.0° of latitude and 2.0° of longitude. These data cover the period from 1958 to 2010 in this study.

Monthly mean of latent heat flux and sensible heat flux data of Japan 25-year Reanalysis (JRA-25) and JMA Climate Data Assimilation System (JCDAS) were used to examine the atmosphere-ocean interaction. The datasets were provided from the cooperative research project of the JRA-25 long-term reanalysis by the Japan Meteorological Agency (JMA) and the Central Research Institute of Electric Power Industry (CRIEPI). The spatial resolution is global grid of 2.5° of latitude and 2.5° of longitude. These data cover the period from 1979 to 2010 in this study.

We analyzed large-scale atmosphere fields, SST fields and thermal transport fields for the period from December 2009 to August 2010. Anomaly fields are calculated from the climatology that is the multi-year average value for each monthly mean. The number of the years for the average depends on the length of the year in each valuable.

Figure 1 obviously shows that the value of the AO index was continuously and extremely positive for the period from 10 July to 4 August 10. We, therefore, define the period as the AO anomalous positive days. Time-mean values of the atmospheric fields are analyzes for this period in detail. The multi-year averaged climatology for the positive days is weighted mean values as

$$\left(\begin{array}{c}\text{The multi year average value of July } \times 22 \\ + \\ \text{The multi year average value of August} \times 4\end{array}\right) \Big/ 26 \, .$$

Chapter 3 Result

3-1. Positive days

First, we demonstrated time-mean atmospheric fields during the extremely positive AO days. The temperature anomaly field of the 850-hPa level obviously showed that a hot anomaly area covered the Japan (Figure 2). In addition, the extremely hot anomaly covered western Russia and the East area of the northern Eurasian continent. Adversely, the extremely cold anomaly covered north polar region and Russian central part. Figure 3 shows 300-hPa geopotential field and the wave activity flux defined by *Takaya and Nakamura* (2001). The 300-hPa height pattern showed negative anomaly over north polar region, whereas positive anomalies covered in mid-latitude in the Northern Hemisphere. This pattern resembles the positive summer AO pattern that was pointed out by *Ogi et al.* (2005). In particular, Russian eastern part, southern and eastern parts of Siberia and northern Pacific Ocean were covered the strong positive anomalies. The negative anomaly covered from northern part of Greenland to northern part of Siberia. Also Japan was covered the positive anomaly. The contour line of the geopotenntial height widely meandered, so that the polar jet stream meandered. The arrow heads of the 300-hPa the wave activity flux overall oriented from Europe to the south of Alaska along the longitudinal circle over the polar jet. The flux of the European eastern part and the eastern part of Siberia was strong. Figure 4 shows the zonal mean value of the westerly wind component in the Northern Hemisphere along with that over 135E. This figure obviously shows the positive anomaly in high latitude, so the double jet stream structure overall the Northern Hemisphere, and over Japan as well.

The OLR over the Atlantic Ocean showed the negative anomaly in the Caribbean Ocean (Figure 5). Since the OLR in the tropics represents convective cloud activity, this negative OLR anomaly implies the existence of high clouds over this area. The velocity potential of 0.995-sigma showed positive values over around the Central America, and anomaly field showed the negative. Additionally, the velocity potential of 0.2582-sigma showed negative values was also located in around Central America, and also anomaly field showed the positive (Figure 6). The omega of 500-hPa height showed upward flow also over the Central America and downward flow over the eastern part of European (Figure 7). Also, anomalies field showed the negative around Central America, and the positive around the eastern part of European.

3-2. A half year time variability of the atmosphere and the ocean

The positive anomaly of the SST persisted over the Atlantic Ocean around 20N from December through August. In association with this SST anomaly, the total anomaly of the latent heat and sensible heat flux showed the negative anomaly in the same place from December to April. However, the anomaly sign changed from the negative to the positive in May, then this positive anomaly continued until August (Figure 8 and 9).

The 300-hPa geopotential height of three months average from 2009 December to 2010 February showed the positive anomaly over Greenland, and showed the negative anomaly over Atlantic, Central Asia and North Pacific Ocean (Figure 10). This is obviously shows a typical negative wintertime AO pattern.

Chapter 4 Discussion and remarks

We examined reversal of Arctic Oscillation pattern from 2009 December through 2010 August, and its relation to the abnormal hot summer. Since the AO index in 2009/2010 winter is strongly negative, the horizontal pattern of the 300-hPa geopotential height of the winter average shows a typical negative AO pattern. We can reconfirm that negative AO pattern appeared in winter. From December to April, the total anomaly of the latent heat and sensible heat flux over the Atlantic Ocean around 20N was downward, i.e., heat transport from the atmosphere to the ocean. In association with this flux anomaly, the anomaly of SST showed the positive in the same region. From winter through spring, the atmosphere made the ocean warm in the Atlantic Ocean around 20N owing to the strong negative AO. The orientation of the heat transport anomaly that is from the atmosphere to the ocean ended in April. From May, the total anomaly of the latent heat and sensible heat flux was from the ocean to the atmosphere in the same area. Also, the anomaly of SST showed the positive in the same area, continuously. This condition lasted from May to August so that the ocean made the atmosphere warm from May to August.

The velocity potential of 0.995-sigma in the positive days showed the convergence around the Central America in the lower troposphere, and the velocity potential of 0.2582-sigma in the positive days showed the divergence around the Central America in upper troposphere. The 500-hPa omega field in the positive days showed upward flow over the Central America and downward flow over the eastern part of European. In addition, the OLR over the Atlantic Ocean in the positive days implied the existence of high clouds over this area. The atmosphere which was warmed in the ocean of the Central America in the lower troposphere converged, and the convection strengthened. In addition, the divergence occurred in the upper troposphere. Also, the upper atmosphere that up drafted over the Central America might arrive over the eastern part of European, and go downward in this region.

The 850-hPa of the temperature in the positive days showed abnormal hot areas. The 300-hPa geopotential height in the positive days resembled the positive AO pattern. The 300-hPa wave activity flux showed Rossby wave propagation from Eurasia of eastern and western parts and the northern Pacific. Additionally, the meandering of the polar jet stream and the double jet appeared. Therefore, the condition in the positive days kept the positive AO pattern.

Therefore, we could confirm the phenomenon of the hypothesis, and show the serial of track. The winter strong negative AO warmed SST in the Atlantic Ocean in low-latitude. The warm SST warmed the atmosphere and strengthened upward motion. Then, the anticyclone was formed over the eastern part of European and the polar jet stream meander. The anticyclone was held over Japan in a long time due to the polar jet stream meandering, and the positive AO pattern was kept in a long time. We found the possibility that the winter strong negative AO affects the summer positive AO. The reversal of AO pattern may be adduced the cause that Japan experienced the abnormal hot summer, and also the area covered anticyclone experienced the abnormal hot summer in 2010. In this study, we analyzed AO pattern in 2009/2010. If the hypothesis can be applied in another year, we may be possible to forecast the abnormal hot summer from an early stage. This is our future study.

Acknowledgment

I learned basic knowledge of the physics and detailed knowledge of the physical oceanography, the atmospheric dynamics and the statistics analysis methods from many professors of Geosystem Science, Department of Environmental Science & Technology, Faculty of Bioresource, Mie University. In addition they gave me advices and help of the coalition seminar. So I thank the professors. Particularly, the professor Yoshihiro Tachibana informed me of detailed knowledge about the atmosphere, data analytical method and the way of the presentation. I express the will of thanks heartily. I thank Dr. Tetsu Nakamura of the Atmospheric Physics Section, Atmospheric Environment Division, National Institute for Environmental Studies, Japan, who taught me the EOF analysis of SV NAM and the wave activity flux. Additionally, the senior associate in Climate and Ecosystems Dynamics Division taught me the way of the student life, how to approach computer and how to compose of the program. In addition, I had they correct argument. I encouraged each other with the classmate and was able to enhance. I express the will of the thanks heartily.

References

Kalnay, E., et al. (1996), The NCEP/NCAR 40-year Reanalysis Project, *Bull. Amer. Meteor. Soc.*, **77**, 437-471.

Liebmann, B., and C. A. Smith (1996), Description of a complete (Interpolated) outgoing longwave radiation dataset, *Bull. Amer. Meteor. Soc.*, **77**, 1275-1277.

Ogi, M., K. Yamazaki, and Y. Tachibana (2004), The summertime annular mode in the Northern Hemisphere and its linkage to the winter mode, *J. Geophys. Res.*, **109**, D20114, doi:10.1029/2004JD004514.

Ogi, M., K. Yamazaki, and Y. Tachibana (2005), The summer northern annular mode and abnormal summer weather in 2003, *Geophys. Res. Lett.*, **32**, L04706, doi:10.1029/2004GL021528.

Smith, T. M., R. W. Reynolds, T. C. Peterson, and J. Lawrimore (2008), Improvements to NOAA's historical merged land-ocean surface temperature analysis (1880−2006), *J. Climate*, **21**, 2283−2296.

Tachibana, Y., T. Nakamura, H. Komiya, and M. Takahashi (2010), Abrupt evolution of the summer Northern Hemisphere annular mode and its association with blocking, *J. Geophys. Res.*, **115**, D12125, doi:10.1029/2009JD012894.

Takaya, K., and H. Nakamura (2001), A formulation of a phase-independent wave-activity flux for stationary and migratory quasigeostrophic eddies on a zonally varying basic flow, *J. Atmos. Sci.*, **58**, 608-627.

Tanimoto, Y., and S.-P. Xie (2002), Inter-hemispheric decadal variations in SST, surface wind, heat flux and cloud cover over the Atlantic Ocean. *J. Meteor. Soc. Japan*, **80,** 1199–1219.

Thompson, D. W. J., and J. M. Wallace (2000), Annular modes in the extratropical circulation. Part I: Month-to-month variability, *J. Clim.*, **13**, 1000–1016.

Wang, L., and W. Chen (2010), Downward Arctic Oscillation signal associated with moderate weak stratospheric polar vortex and the cold December 2009, *Geophys. Res. Lett.*, **37**, L09707, doi: 10.1029/2010GL042659.

Xue, Y., T. M. Smith, and R. W. Reynolds (2003), Interdecadal changes of 30-yr SST normals during 1871–2000, *J. Climate*, **16,** 1601–1612.

Figure captions

Figure 1 Daily variation of the SV NAM index from 2009 November to 2010 August. The abscissa axis shows dates, and the vertical axis shows the SV NAM index.

Figure 2 The 850-hPa temperature [K] in the positive days (shade: anomaly, contour: average).

Figure 3 The 300-hPa geopotential height [m] and the wave activity flux [m^2 s^{-2}] in the positive days (shade: geopotential anomaly, contour: geopotential average, arrow: wave activity flux).

Figure 4 Vertical cross-section of the eastward component of the wind [m s^{-1}] at 135E in the Northern Hemisphere in the positive days (shade: anomaly, contour: average). The abscissa axis shows latitude, and the vertical axis shows levels.

Figure 5 The OLR [W m^{-2}] in the positive days (shade: anomaly, contour: average).

Figure 6 The velocity potential [1×10^6 m^2 s^{-1}] in the positive days (bottom: 0.995-sigma, top: 0.2582-sigma, shade: anomaly, contour: average).

Figure 7 The 500-hPa omega [1×10^{-2} P s^{-1}] in the positive days (shade: anomaly, contour: average).

Figure 8 Monthly average SST [ºC] (left) and the total of latent heat flux and sensible heat flux [W m^{-2}] (right) from (top) 2009 December to (bottom) 2010 April (shade: anomaly, contour: average).

Figure 9 Monthly average SST [ºC] (left) and the total of latent heat flux and sensible heat flux [W m^{-2}] (right) from (top) 2010 May to (bottom) 2010 August (shade: anomaly, contour: average).

Figure 10 The 300-hPa geopotential height [m] of the three months average from December 2009 to February 2010 (shade: anomaly, contour: average).

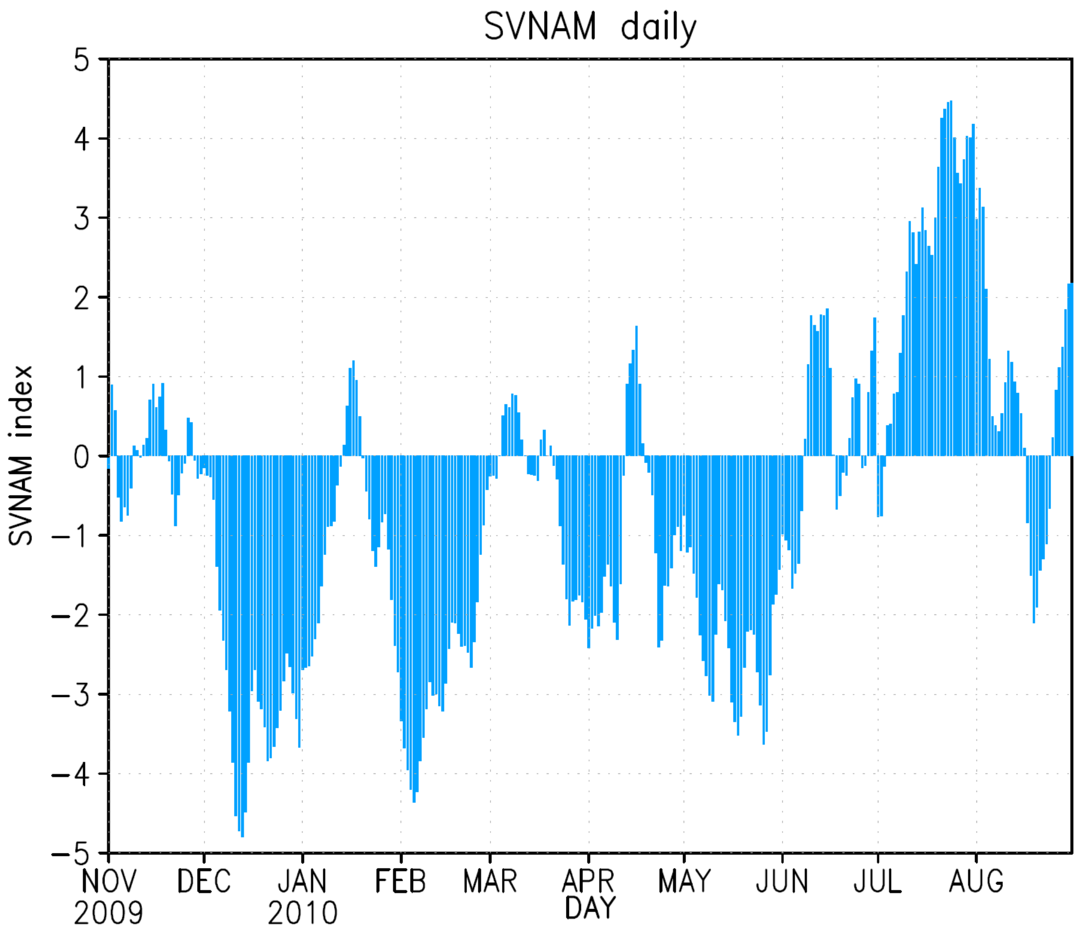

Figure 1 Daily variation of the SV NAM index from 2009 November to 2010 August. The abscissa axis shows dates, and the vertical axis shows the SV NAM index.

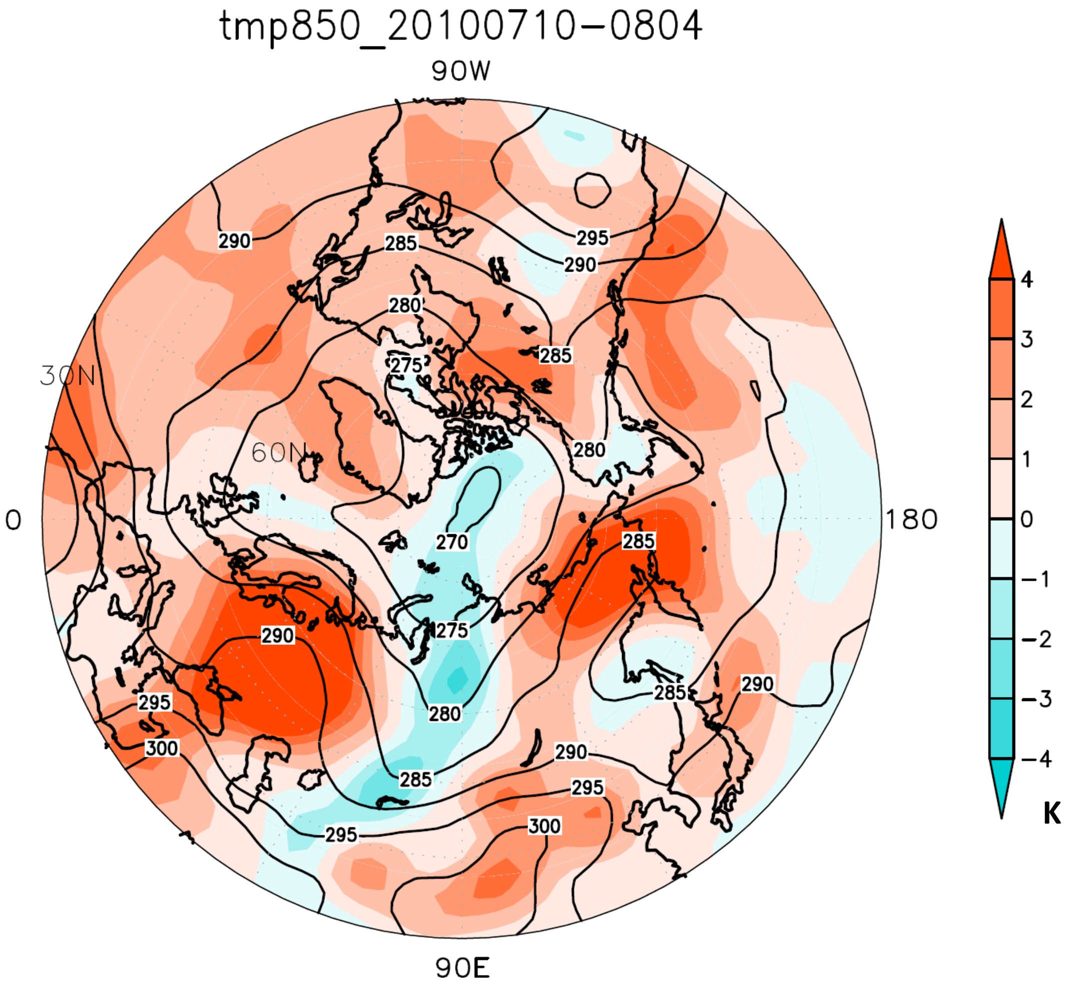

Figure 2 The 850-hPa temperature [K] in the positive days (shade: anomaly, contour: average).

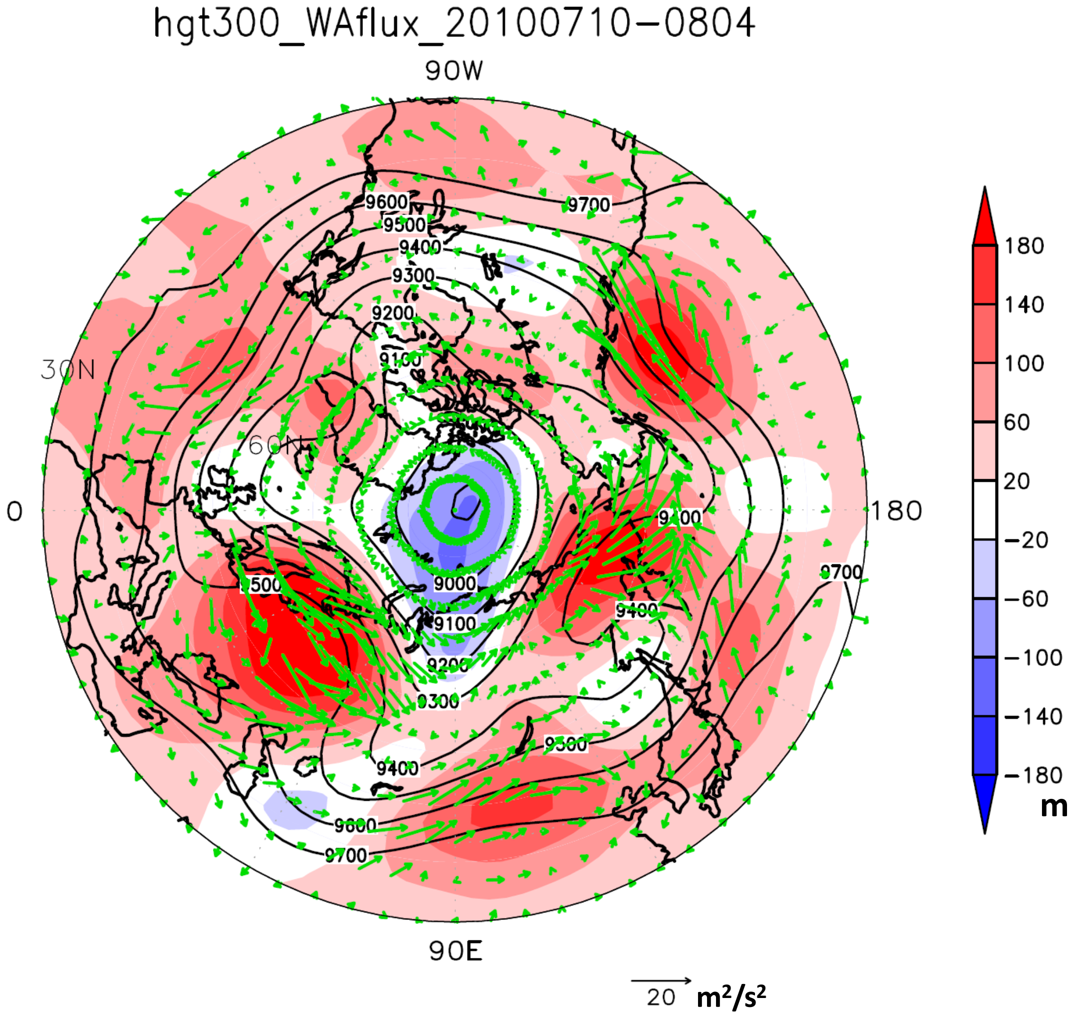

Figure 3 The 300-hPa geopotential height [m] and the wave activity flux [m^2 s^{-2}] in the positive days (shade: geopotential anomaly, contour: geopotential average, arrow: wave activity flux).

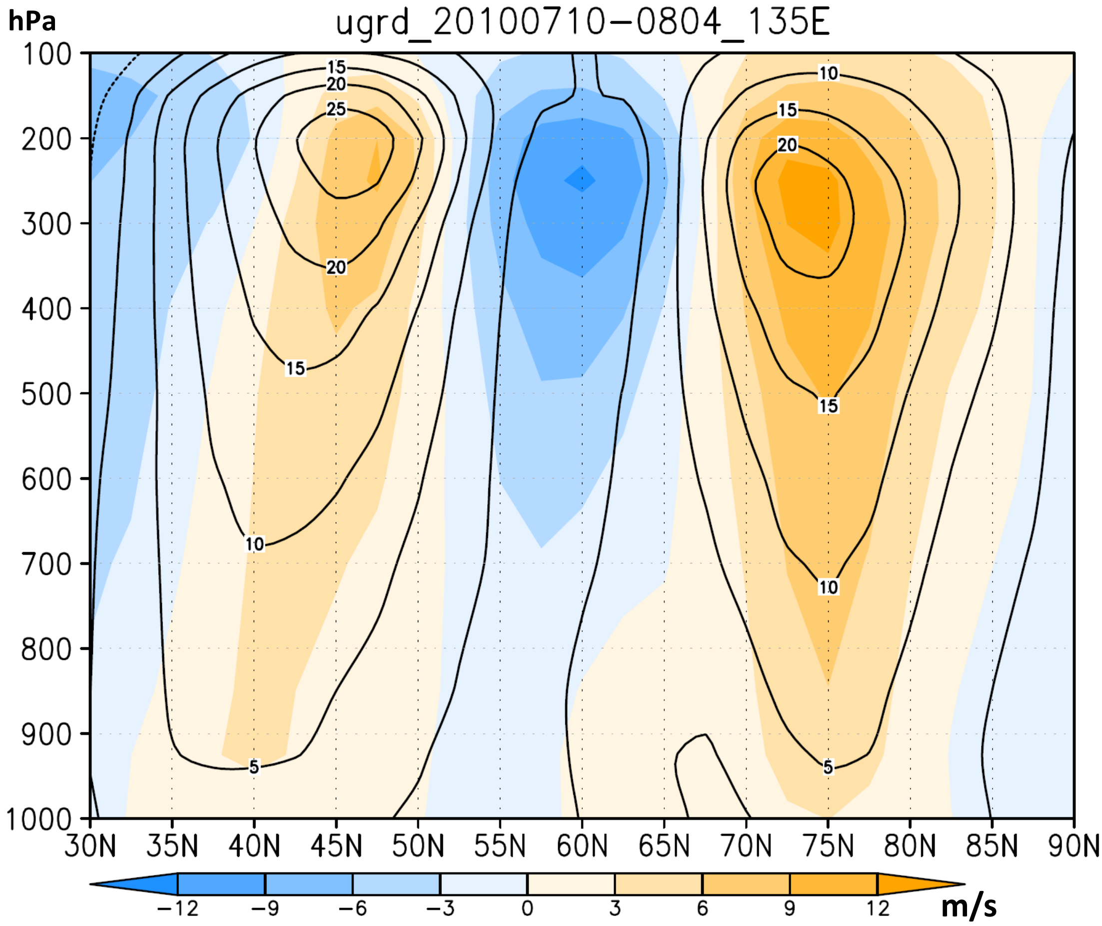

Figure 4 **Vertical cross-section of the eastward component of the wind [m s[-1]] at 135E in the Northern Hemisphere in the positive days (shade: anomaly, contour: average). The abscissa axis shows latitude, and the vertical axis shows levels.**

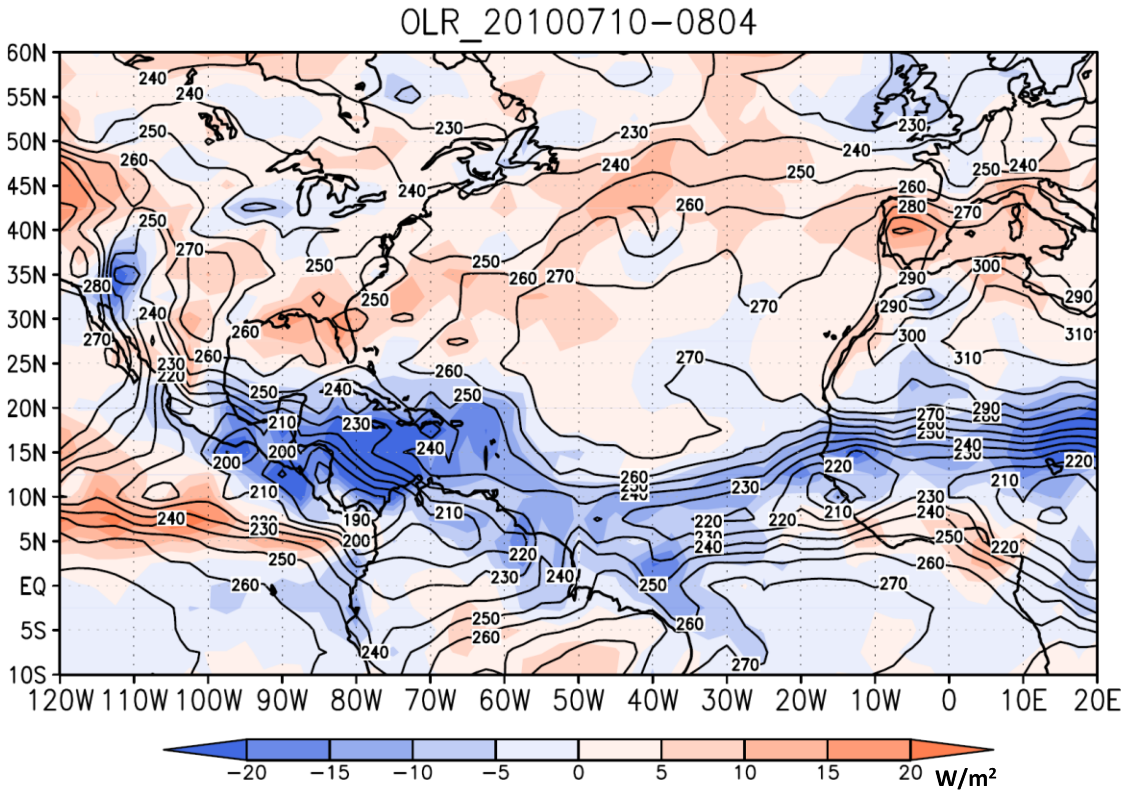

Figure 5 The OLR [W m^{-2}] in the positive days (shade: anomaly, contour: average).

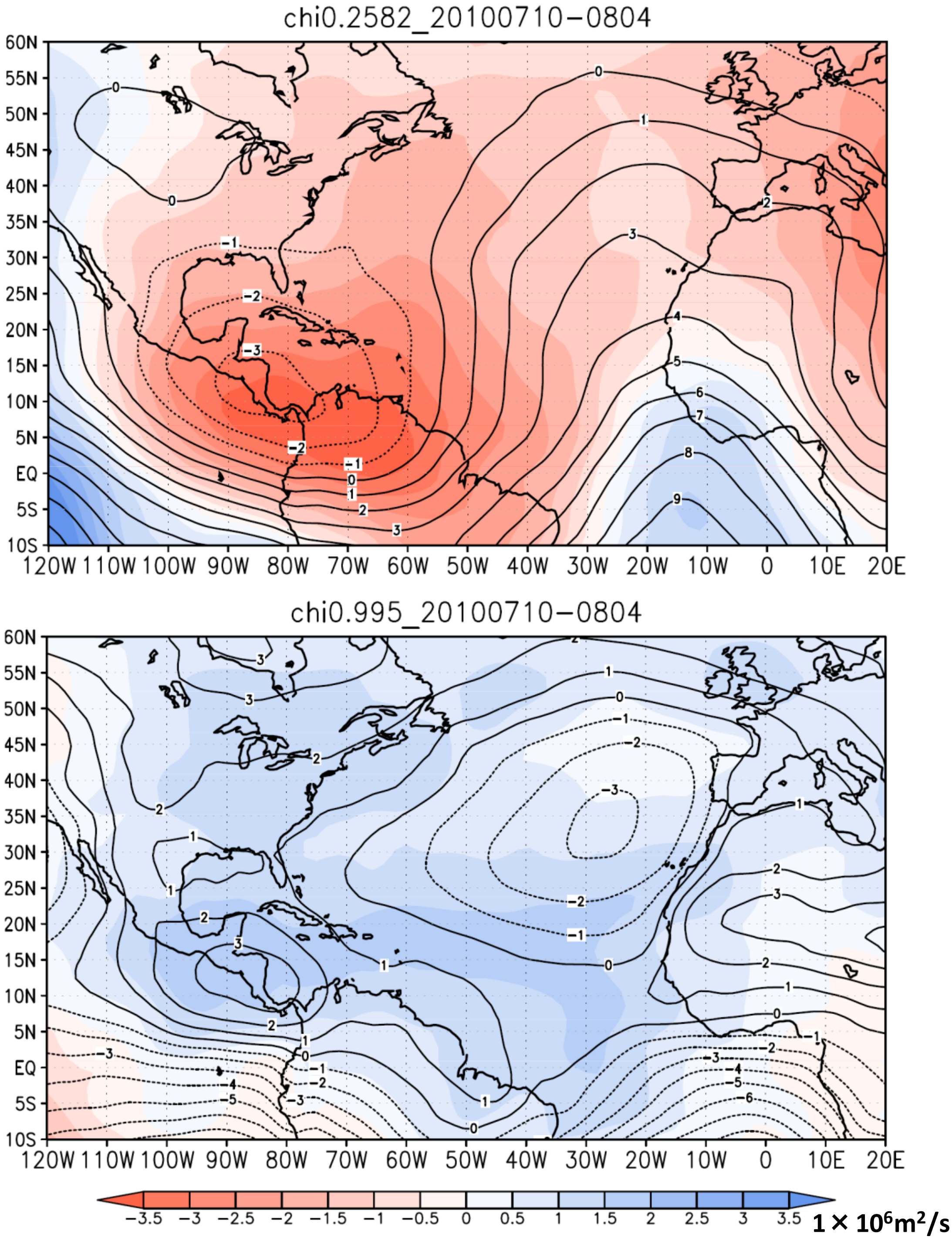

Figure 6 **The velocity potential [1×10^6 m^2 s^{-1}] in the positive days (bottom: 0.995-sigma, top: 0.2582-sigma, shade: anomaly, contour: average).**

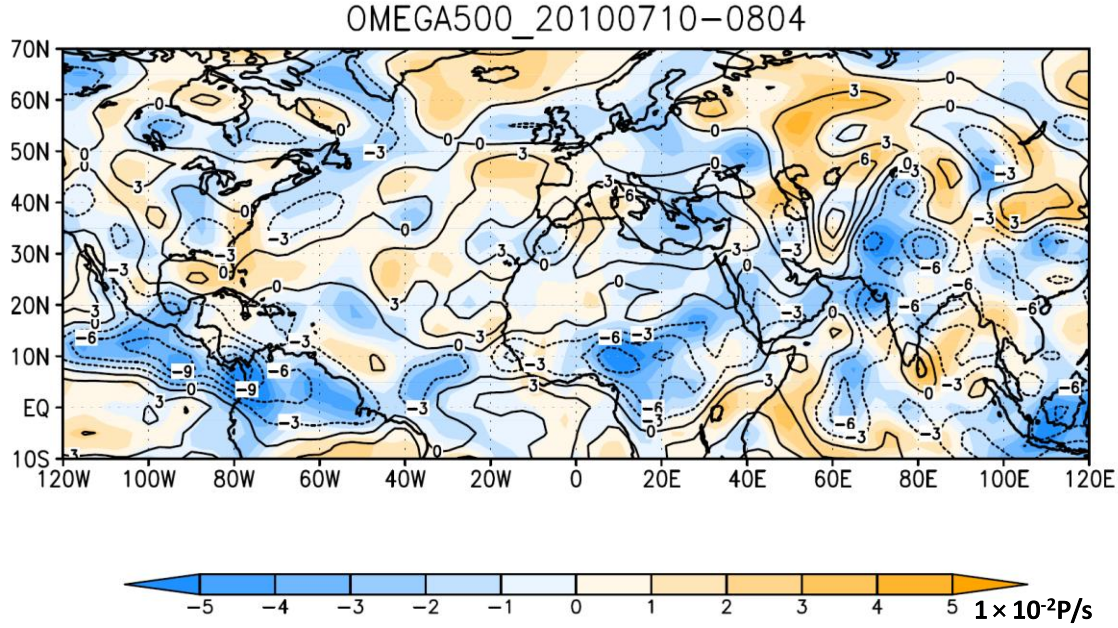

Figure 7　The 500-hPa omega [1×10^{-2} P s^{-1}] in the positive days (shade: anomaly, contour: average).

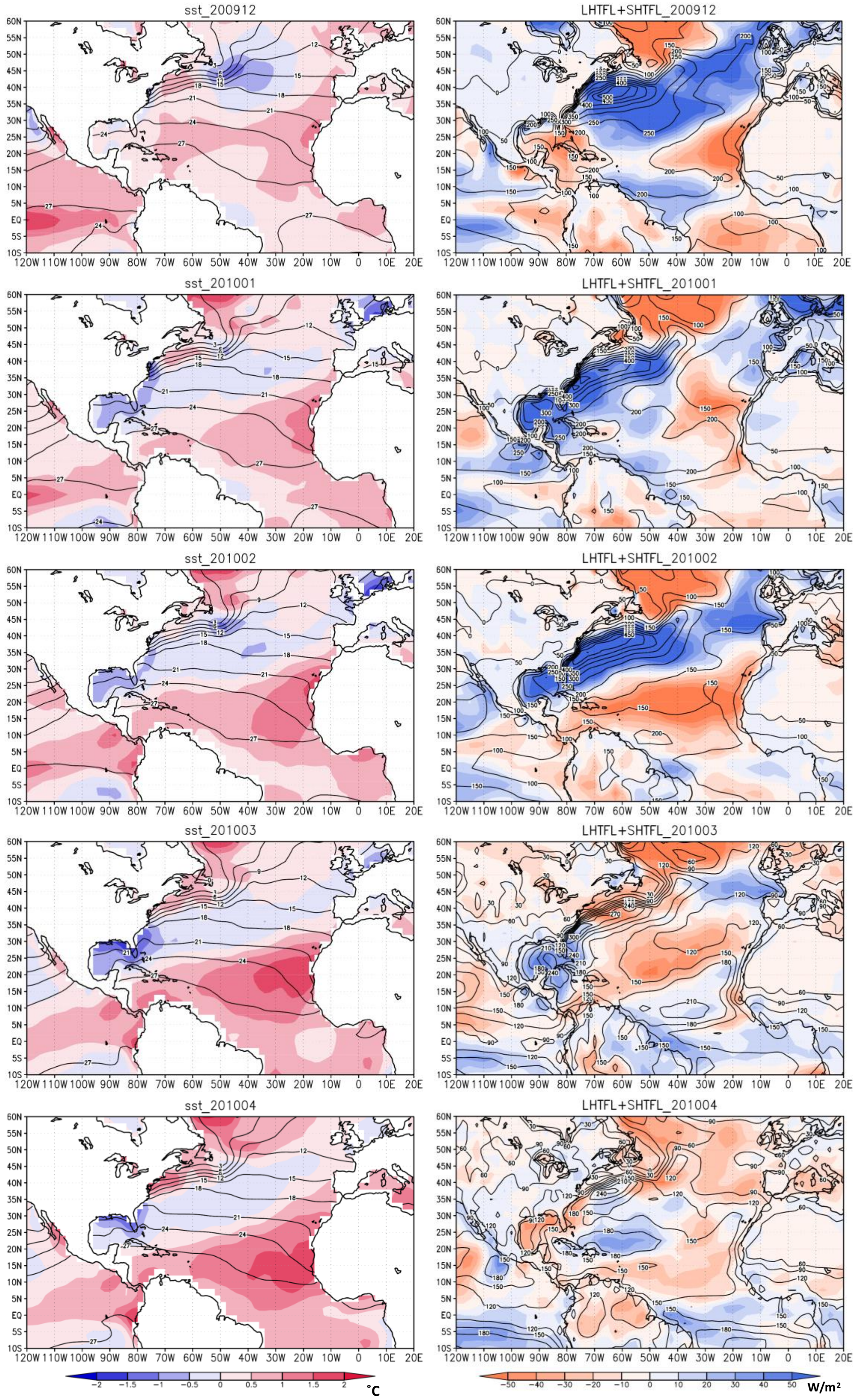

Figure 8 Monthly average SST [°C] (left) and the total of latent heat flux and sensible heat flux [W m^{-2}] (right) from (top) 2009 December to (bottom) 2010 April (shade: anomaly, contour: average).

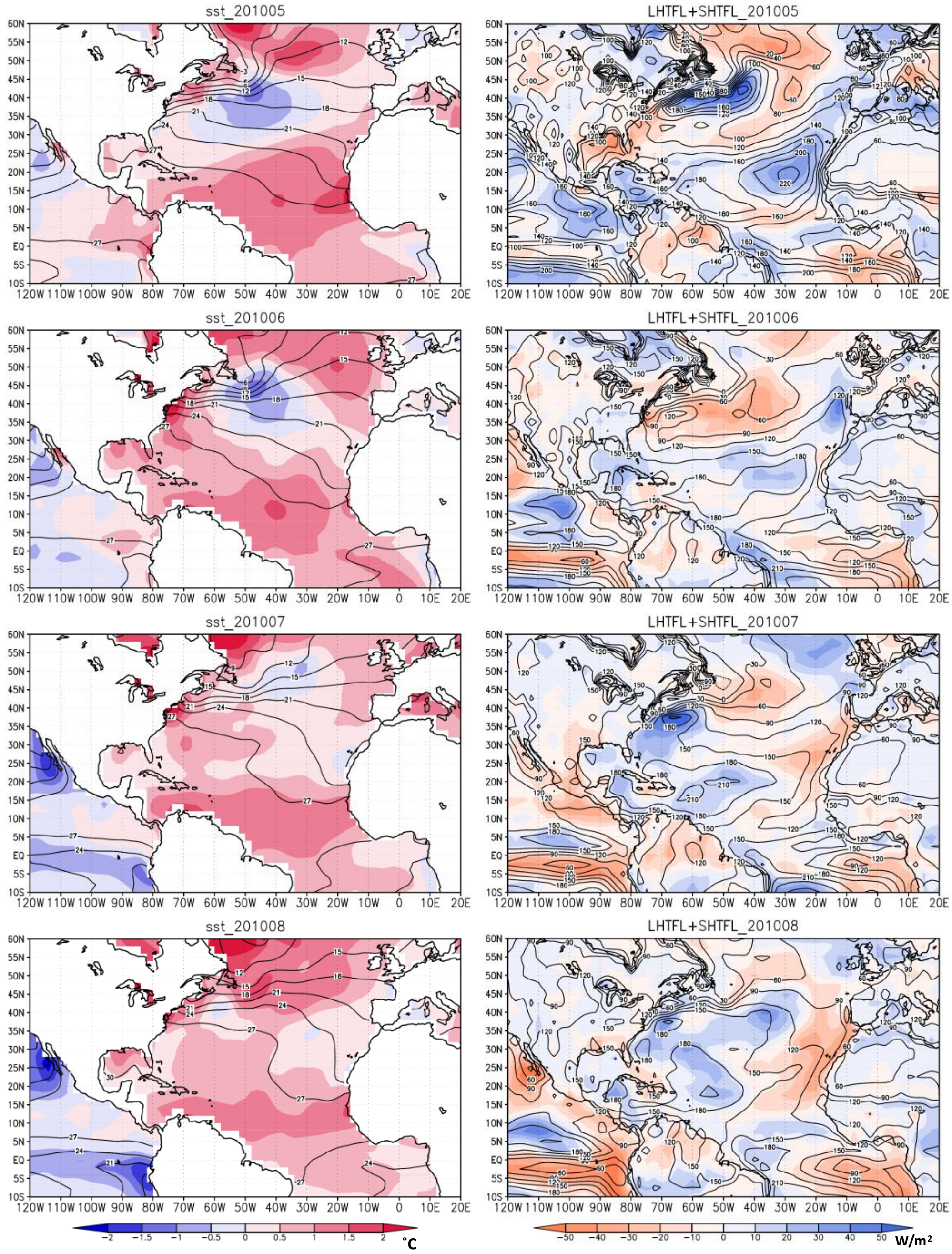

Figure 9 Monthly average SST [ºC] (left) and the total of latent heat flux and sensible heat flux [W m^{-2}] (right) from (top) 2010 May to (bottom) 2010 August (shade: anomaly, contour: average).

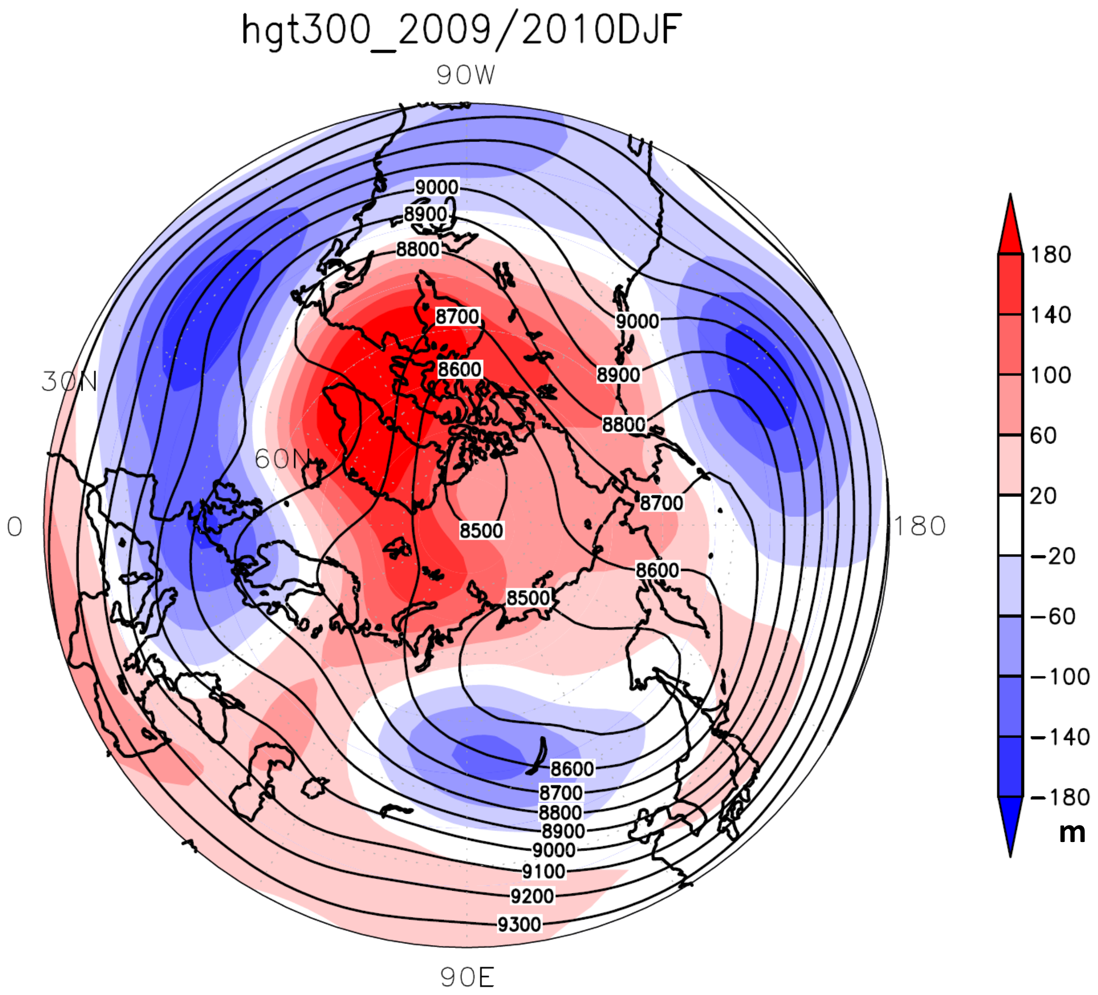

Figure 10　The 300-hPa geopotential height [m] of the three months average from December 2009 to February 2010 (shade: anomaly, contour: average).